PHYSICAL REVIEW B VOLUME 26, NUMBER 10 15 NOVEMBER 1982

Raman studies of benzene-derived graphite fibers

T. C. Chieu and M. S. Dresselhaus
Department of Electrical Engineering and Computer Science, and Center for Materials Science and Engineering, Massachusetts Institute of Technology, Cambridge, Massachusetts 02139

M. Endo
Faculty of Engineering, Shinshu University, Nagano 380, Japan
(Received 26 April 1982)

Carbon fibers prepared from thermal decomposition of benzene at ~1100 °C are studied by Raman spectroscopy as a function of heat-treatment temperature. The structural ordering at each heat-treatment temperature is monitored by observation of both the Raman-allowed E_{2g_2} mode at 1580 cm^{-1} and the disorder-induced lines at ~1360 cm^{-1} in the first-order spectra and at 2730 and 2970 cm^{-1} in the second-order spectra. Raman and resistivity results indicate three characteristic heat-treatment temperatures relevant to the establishment of in-plane and interplanar ordering. Using fibers heat treated to the maximum available temperature of 2900 °C, Raman spectroscopy shows that single-staged fibers can be prepared by acceptor intercalation, in agreement with direct Debye-Scherrer x-ray measurements. Resistivity measurements on pristine fibers previously heat treated to 2900 °C show a metallic temperature dependence with $\rho = 70\ \mu\Omega$ cm at 300 K and a residual resistance ratio of 1.5. Upon intercalation, a resistivity $\rho = 7\ \mu\Omega$ cm at 300 K and a residual resistance ratio of 5 is achieved. Raman-spectroscopy and temperature-dependent resistivity measurements demonstrate that the benzene-derived fibers exhibit the highest degree of ordering achieved in fibers and provide an attractive host material for intercalation.

I. INTRODUCTION

By heat treatment of carbon fibers prepared by the pyrolysis of benzene, graphite fibers of unusually high structural order, high electrical conductivity, and high bulk-modulus and tensile strength have been prepared.[1,2] These fibers have been characterized by a variety of techniques such as electron microscopy,[3,4] x-ray diffraction,[3,5] resistivity measurements,[5,6] magnetoresistance studies[7] and studies of mechanical properties.[5] In all cases, the characterization methods have confirmed the high degree of structural perfection that can be obtained by heat treatment of these fibers to ~2900 °C.

Until now, no measurements of the lattice modes of these materials have been reported, though measurements of lattice modes by Raman spectroscopy have been shown to provide a sensitive method for the characterization of the structural perfection of carbon fibers.[8,9] Since the benzene-derived fibers are typically between 10 and 20 μm in diameter, Raman spectroscopy can be used to examine the structure within the optical skin depth (~600 Å for light scattering at 4880 Å), thereby providing a complementary tool to x-ray diffraction, resistivity, and magnetoresistance techniques which are sensitive to the bulk fiber. In this work, Raman spectroscopy is used to characterize (as a function of heat-treatment temperature) the optical skin depth of carbon fibers prepared by the pyrolysis of benzene. It is shown that by heat treatment to ~2900 °C the lattice mode structure within the optical skin depth exhibits a high degree of structural perfection, consistent with the application of other characterization techniques to these fibers.

Raman spectroscopy is a useful technique for the characterization of crystalline perfection because Raman scattering from perfect crystals is limited to contributions from Raman-active zone-center modes. In disordered systems, the crystallite size becomes much less than the optical wavelength, and the selection rule restricting Raman scattering to essentially zone-center modes is relaxed. Thus for disordered systems, contributions from other phonons in the Brillouin zone become possible, in particular at phonon frequencies where there are maxima in the phonon density of states and the coupling to the incident electromagnetic radiation is large. Several features in the first- and second-order Raman spectra for disordered graphites can thus be

used to characterize carbon fibers. In this way, a correlation is obtained between the heat-treatment temperature and the degree of structural perfection that is achieved in the fiber.

In the first-order spectrum, the most important disorder-induced change is the appearance of a disorder-induced line peaking at ~ 1360 cm^{-1} and associated with a large density of phonon states. In particular, Tuinstra and Koenig[8] have noted the linear relation between the inverse of the in-plane crystallite dimension L_a and the ratio $R = I_{1360}/I_{1580}$ of the integrated intensity of the disorder-induced line at 1360 cm^{-1} to the Raman-allowed line at 1580 cm^{-1}. This allows a quantitative characterization to be made of the degree of disorder in the fibers. In addition, the linewidth and line frequency of the disorder-induced 1360-cm^{-1} line are highly sensitive to disorder in the graphite lattice. Also sensitive to disorder are the linewidth and the peak frequency of the Raman-allowed line near 1580 cm^{-1}. Disorder causes this line to broaden and upshift in frequency, reflecting the high density of phonon states near 1620 cm^{-1} for midzone phonons. In some cases, contributions from the high density of phonon states near 1620 cm^{-1} can be clearly distinguished in the observed Raman spectra for disordered graphite, and the present work shows examples of such spectra.

Likewise, the second-order spectra can be used to characterize disordered graphites. As in the case of the disorder-induced 1360-cm^{-1} line in the first-order spectrum, there is a disorder-induced line in the second-order spectrum peaking at ~ 2970 cm^{-1} and associated with a combination mode between the peaks in the phonon density of states at ~ 1360 cm^{-1} due predominantly to zone-edge phonons and also at ~ 1620 cm^{-1} due predominantly to midzone phonons.[10] In this case, the intensity, linewidth, and line frequency are all sensitive to disorder. In addition, disorder-induced changes are observed in the lines normally found in the second-order spectrum for single-crystal graphite flakes, associated primarily with the main peak at ~ 2730 cm^{-1} which exhibits an additional feature at ~ 2700 cm^{-1} in the most perfectly ordered samples. This feature is observed in highly oriented pyrolytic graphite (HOPG) stress annealed at 3600 °C. In the present work, it is shown that this feature is also seen in the Raman spectra for the benzene-derived fibers heat treated to 2900 °C.

Recent Raman studies of the graphitization of carbon-carbon composites by high-temperature heat treatment[11] and of the effect of ion implantation and subsequent annealing on the graphite lattice[12–14] have shown that specific features of the Raman spectra are particularly sensitive to specific aspects of the lowering of crystalline order, such as the in-plane crystallite size, the onset of three-dimensional ordering, and the establishment of long-range three-dimensional ordering. The present work shows this aspect of Raman spectroscopy to be equally applicable to the characterization of the heat-treatment process in carbon fibers. The results obtained are in excellent agreement with other studies of the graphitization process[11,15] showing that in-plane ordering is established by heat treatment to ~ 2000 °C, while heat treatment above 2600 °C is required for the onset of three-dimensional ordering. At the highest heat-treatment temperature of 2900 °C, the Raman spectrum for the benzene-derived fibers is nearly identical to that of HOPG, consistent with a much higher degree of ordering than has been previously reported for any graphite fiber.[8,9,16]

A summary of the experimental procedures used in the preparation of the materials and in the measurements themselves is given in Sec. II. Section III presents results for the first- and second-order Raman spectra and the electrical resistivity for a range of heat-treatment temperatures. The interpretation of these experimental measurements are related to results on similar fibers obtained by other techniques. A comparison is also given between the present results and those obtained by other Raman studies of graphite fibers,[8,9,16] as well as with other studies using Raman scattering to investigate the graphitization process.[11,15]

Raman spectroscopy was also used to study the effect of intercalation on the modification of the pristine fibers and to characterize the staging of the fibers within the optical skin depth, employing the same techniques as were previously developed.[16] Resistivity measurements were used to characterize the specific fibers used in the present study, by comparison with previous resistivity results on similarly prepared fibers.[5,6] The temperature dependence of the resistivity was also measured, providing information about charge-carrier-scattering mechanisms in the fibers. In addition temperature-dependent resistivity measurements are reported for intercalated fibers previously heat treated to 2900 °C.

II. EXPERIMENTAL PROCEDURES

The original carbon fibers used in the present investigation were prepared on a substrate by pyrolyz-

ing a mixture of benzene and hydrogen at a temperature of 1100°C. Graphitization of the fibers is accomplished by heat treatment at various temperatures from 1300 to 2900°C, using a carbon-resistance furnace in a high-purity argon atmosphere. The residence time at the desired temperature of the heat treatment was 30 min and the heat-treatment temperature was measured to an accuracy of $\pm 1\%$ by a high-temperature optical pyrometer focused on the fiber samples.

The resulting fibers consist of concentric graphite layers around the fiber axis, such as annular rings of a tree.[1,2] The fiber diameters used in this work were in the range from 10 to 20 μm, but were constant to $\pm 5\%$ along the fiber axis of a single fiber several centimeters in length. With this technique it is possible to make fibers of much smaller diameter (down to ~ 5000 Å) which are of great interest for other types of experiments, but such small diameter fibers were not used in the present work.

The Raman scattering measurements used to monitor the heat treatment were made at room temperature in the backscattering configuration using a cylindrical lens to focus the 4880-Å argon-ion laser beam (~ 50 mW) and a double monochromator to measure the frequency shift. The output signal at the photomultiplier tube was collected using a photon counter and a multichannel analyzer.

The electrical resistivity of single fibers was measured by a conventional four-terminal method[17] with a dc current of 1 mA. The electrical contacts between the samples and lead wires were made using silver paint. The samples were cut into about 15-mm lengths and the diameter of each sample was measured by an optical microscope. The temperature-dependent resistivity measurements were carried out between room temperature and liquid-helium temperatures.

Only the fibers heat treated to the highest heat-treatment temperature of 2900°C were intercalated with the alkali-metal donor Rb and acceptors $FeCl_3$ and $AlCl_3$ using previously developed techniques for the intercalation of fibers.[9] Raman scattering measurements were also carried out on intercalated graphite fibers which were encapsulated in glass ampoules to prevent intercalate desorption.

III. RESULTS AND DISCUSSION

A. Raman spectroscopy

The first-order Raman spectra of the fibers heat treated at various heat-treatment temperatures (T_{HT}'s) are shown in Fig. 1. Two main Raman modes are generally observed in these spectra, one at about 1580 cm^{-1} which corresponds to the Raman-allowed E_{2g_2} mode in HOPG, and one at about 1360 cm^{-1} which corresponds to the disorder-induced line. The latter is associated with an intense peak in the phonon density of states, is known to occur in many less-ordered carbons, is structure sensitive, and is absent in the spectra of graphite single crystals and HOPG.[8] A weak structure is also found near 1620 cm^{-1} (dashed lines) and is identified with a large phonon density of states associated with midzone phonons.

As T_{HT} is increased, distinct differences in these spectra are observed with regard to the ratio of the integrated intensities of the Raman peaks $R = I_{1360}/I_{1580}$, the line frequencies and linewidths of the lines at 1360 and 1580 cm^{-1}. Of particular

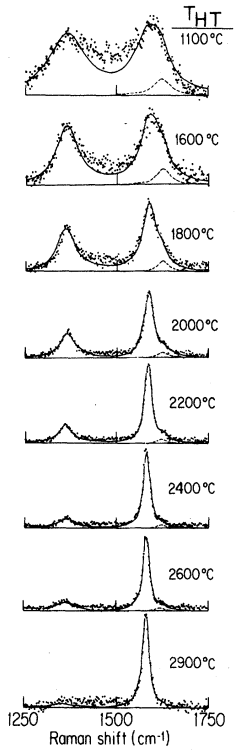

FIG. 1. First-order Raman spectra for benzene-derived carbon fibers heat treated at various heat-treatment temperatures (T_{HT}). As T_{HT} is increased, the intensity of the disorder-induced line at ~ 1360 cm^{-1} decreases and the linewidth of the Raman-allowed line decreases. At the highest T_{HT} used in the present work (2900°C), the line at ~ 1360 cm^{-1} can barely be detected. Solid lines represent a Lorentzian fit to the experimental points. Dashed lines represent a Lorentzian fit to a line at ~ 1620 cm^{-1}.

interest is the dramatic decrease in R and the decrease in linewidth with increasing T_{HT}, indicating that defect structures originally present in these fibers are gradually healed as the T_{HT} increases and that the ordered three-dimensional graphite crystal structure is progressively formed. The spectrum for $T_{HT} \simeq 2900$ °C is nearly identical in position and width to that for HOPG.

Figure 2 shows a plot of the ratio of the relative intensity of the Raman lines $R = I_{1360}/I_{1580}$ as a function of T_{HT}. Since the ratio R varies as the inverse of the average crystal planar domain size, L_a,[8] we have used this result to estimate the domain size for the Raman spectra shown in Fig. 1. A plot of L_a vs T_{HT} obtained in this way is also presented in Fig. 2 (right-hand scale). From our data in Fig. 2, it follows that the intensity ratio $R = I_{1360}/I_{1580}$ generally decreases with increasing T_{HT}. For $T_{HT} \leq 1700$ °C, the decrease is relatively slow, but becomes much faster for $1700 \leq T_{HT} \leq 2400$ °C. At the highest T_{HT} used in the present work, $T_{HT} = 2900$ °C, the ratio R is so small that it is difficult to measure accurately (i.e., $R < 0.1$). A value of $R = 0.1$ corresponds to an L_a value of ~ 500 Å. Because of the difficulty in measuring small R values accurately, the first-order Raman spectrum is not a sensitive measurement of L_a for $L_a > 200$ Å.

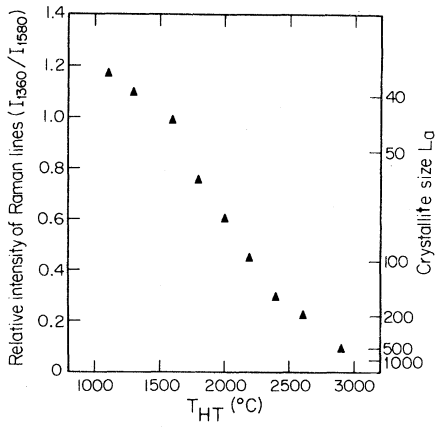

FIG. 2. Plot of the intensity ratio of the disorder-induced line at ~ 1360 cm^{-1} to the Raman-allowed line at ~ 1580 cm^{-1} vs heat-treatment temperature (T_{HT}) for the benzene-derived carbon fibers. On the right scale, the intensity ratio $R = I_{1360}/I_{1580}$ is related to the crystallite size L_a using the results of Ref. 8. The shape of the curve is related to the various steps in the graphitization process (see text).

The variation in line widths [halfwidth at half maximum (HWHM)] as a function of T_{HT} of the 1360- and 1580-cm^{-1} lines is shown in Fig. 3. The mode frequency of the 1580-cm^{-1} line as a function of T_{HT} is shown in Fig. 4. As can be seen in these plots, the heat-treatment process exhibits three regions. The first region corresponds to a T_{HT} below 1700 °C. In this T_{HT} range, the ratio R undergoes a small change and decreases from 1.20 to 0.90, corresponding to a small increase in L_a from 35 to 47 Å, but L_a remains small. In the same temperature range, the linewidths of the two modes narrow significantly. For example, the HWHM intensity $W_{1/2}$ of the 1580-cm^{-1} line decreases from 55 to 20 cm^{-1} (see Fig. 3). In this T_{HT} range where L_a is small, the mode frequency of the 1580-cm^{-1} line undergoes little change but remains upshifted by ~ 15 cm^{-1} with respect to the graphite single-crystal value (see Fig. 4), consistent with the observation of Tuinstra and Koenig.[8]

The second region corresponds to T_{HT} in the range $1800 \leq T_{HT} \leq 2500$ °C. In this T_{HT} range, a sharp decrease in R with increasing T_{HT} is observed. This corresponds to a growth of L_a up to 180 Å for the benzene-derived fibers which is compared to the L_a value of 200 Å reported for the polyacrylonitrile-based (PAN-based) Morganite I fiber.[8] The linewidth (Fig. 3) decreases slowly in this range of T_{HT}, while the mode frequency of the 1580-cm^{-1} line (Fig. 4) decreases rapidly and approaches the value of pristine HOPG. This region corresponds to the establishment of long-range in-

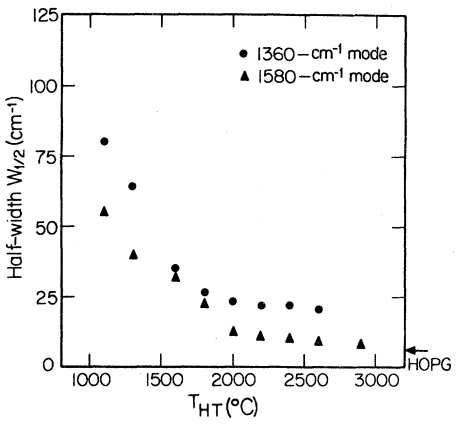

FIG. 3. Plot of halfwidth at half maximum (HWHM) linewidth vs heat-treatment temperature (T_{HT}) for the 1360- and 1580-cm^{-1} Raman lines for the benzene-derived carbon fibers. For $T_{HT} < 1800$ °C, the linewidth HWHM decreases rapidly with increasing T_{HT}. Saturation of HWHM occurs for $T_{HT} \geq 2000$ °C (see text).

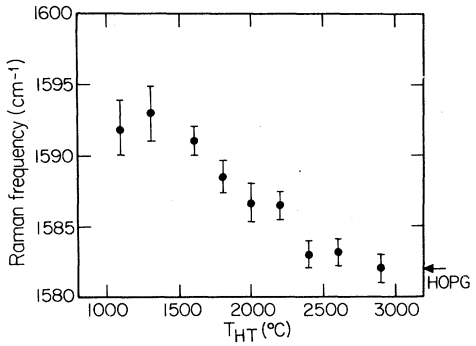

FIG. 4. Plot of the Raman frequency for the dominant peak near ~ 1580 cm^{-1} vs heat-treatment temperature (T_{HT}). At the maximum T_{HT} value used in the present work, the Raman-mode frequency is within 1 cm^{-1} of that of HOPG.

plane order and to a partial development of the three-dimensional graphite structure in the fibers, as also evidenced by the appearance of three-dimensional electron-diffraction spots at a T_{HT} of about 2200 °C (Ref. 3) and by the transition from a negative to a positive transverse magnetoresistance at a T_{HT} above ~ 2100 °C.[7] In this T_{HT} range, the ratio R in Fig. 2 decreases rapidly.

The third region corresponds to T_{HT} above 2600 °C. In this T_{HT} region, the linewidth and mode frequency of the 1580-cm^{-1} line decrease very slowly toward the values of pristine HOPG, while the in-plane crystallite size L_a increases dramatically with T_{HT} and exceeds 500 Å at $T_{HT} = 2900$ °C. This region of T_{HT} corresponds to a nearly complete graphitization of the fibers and a nearly full establishment of three-dimensional graphite ordering. In the third range of T_{HT}, the ratio R of Fig. 2 is very small and decreases slowly to values too small to measure accurately.

In considering the intensity ratio of the two Raman lines one should note that the first-order Raman line near 1580 cm^{-1} for microcrystalline graphite actually consists of a double structure,[10,14] with the main component peaking near 1580 cm^{-1} and an additional weaker feature at about 1620 cm^{-1} (see Fig. 1). The Raman line at 1620 cm^{-1} is sharp and decreases in intensity as T_{HT} increases. Figure 5 shows plots of the dependence on T_{HT} of the relative intensity I_{1620}/I_{1580}, the line frequency and linewidth of the 1620-cm^{-1} line. This additional feature at ~ 1620 cm^{-1} corresponds to a maximum in the phonon density of states[10,18–20] and exhibits a behavior similar to that of the 1360-cm^{-1} disorder-induced line with regard to the change of relative intensity and linewidth with T_{HT}.

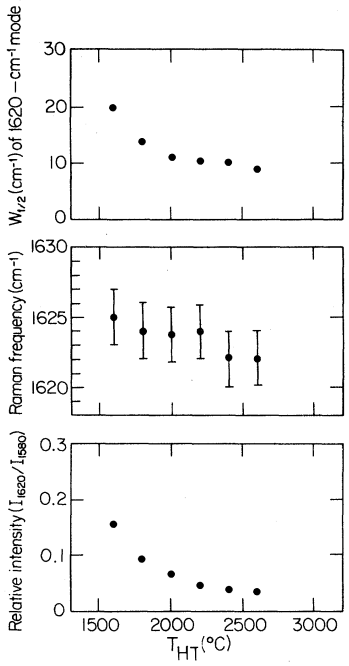

FIG. 5. Dependence on heat-treatment temperature (T_{HT}) of the halfwidth at half maximum (HWHM) linewidth, the mode frequency for the 1620-cm^{-1} disorder-induced mode, and the Raman intensity ratio I_{1620}/I_{1580} for benzene-derived graphite fibers. The 1620-cm^{-1} disorder-induced mode becomes highly attenuated as long-range two-dimensional ordering is established and three-dimensional ordering develops.

This similarity in behavior confirms the similar origin of the feature at ~ 1620 cm^{-1} and the disorder-induced line near 1360 cm^{-1}. We note that the intensity of the 1620 cm^{-1} mode decreases to a unresolvable level for $T_{HT} \sim 2600$ °C, in agreement with the identification of the $T_{HT} \sim 2600$ °C with the establishment of long-range in-plane ordering and significant three-dimensional graphite ordering.

The above conclusions also follow from analysis of the second-order Raman spectra. Characterization studies of lattice disorder in ion-implanted graphite have shown that the second-order Raman spectra are often more sensitive than the first-order spectra to the graphite ordering.[13] Second-order (two-phonon) Raman spectra have been investigated for various types of graphite samples with different in-plane crystallite sizes.[10] The dominant features in the second-order spectrum are a strong line at ~ 2730 cm^{-1} and a weak but sharp feature at ~ 3250 cm^{-1}. In addition a broad feature at ~ 2970 cm^{-1}, which is caused by lattice disorder,

has also been observed in samples of small crystallite sizes.[10] Nemanich and Solin[10] have shown that as the crystallite size increases, the feature at ~ 2730 cm^{-1} becomes narrower, and the feature at ~ 2970 cm^{-1} is suppressed. In contrast, the second-order Raman spectra for single-crystal graphite and pristine HOPG show no structure at 2970 cm^{-1} and a partially resolved doublet structure at 2735 cm^{-1}.[10,11,21]

The identification of these second-order features can be made using the density of phonon states determined on the basis of the graphite phonon dispersion relation.[19,20] The main features in the phonon density of states are peaks near 1360 and 1620 cm^{-1}. Their harmonics at 2×1360 cm$^{-1}=2720$ cm^{-1} and 2×1620 cm$^{-1}=3240$ cm^{-1} correspond, respectively, to the features at 2730 and 3250 cm^{-1} in the second-order spectrum. The disorder-induced line at 2970 cm^{-1} results from the combination of the zone-center 1580-cm^{-1} mode and the zone-edge 1360-cm^{-1} mode.[22,23]

Results for the second-order Raman spectra from the present fibers heat treated at various temperatures are shown in Fig. 6. An intense feature at ~ 2730 cm^{-1} and a weak but sharp feature at ~ 3250 cm^{-1} are observed in all second-order spectra. The 2730-cm^{-1} peak is broad and rather weak at low T_{HT} and increases in peak intensity as the T_{HT} increases. Besides these two features, another broad peak at ~ 2970 cm^{-1} is also observed in the second-order spectra for T_{HT} below 2400 °C. This feature, which is a disorder-induced line, is completely suppressed for $T_{HT} \geq 2600$ °C. The study of these second-order features together with the first-order spectra provides a technique for the characterization of three-dimensional ordering during the heat-treatment process of the fiber samples. When the completion of the graphitization process is achieved, all the line frequencies and linewidths of the main features in the first- and second-order spectra become identical with those of HOPG.

Plots of the linewidth and line frequency of the 2730-cm^{-1} line are shown in Fig. 7. As can be seen from this figure, the line frequency decreases significantly up to a T_{HT} of 2000 °C, then starts to increase slowly and approaches the value of HOPG which is 2735 cm^{-1}. The linewidth (HWHM) decreases rapidly with T_{HT} for $T_{HT} \leq 2000$ °C, and then saturates to a minimum value of 32 cm^{-1} in the range $2000 < T_{HT} < 2200$ °C. The linewidth at the highest T_{HT} of 2900 °C is 30 cm^{-1}, which is to be compared to a HWHM linewidth of 16 cm^{-1} in HOPG. The small increase in linewidth of the

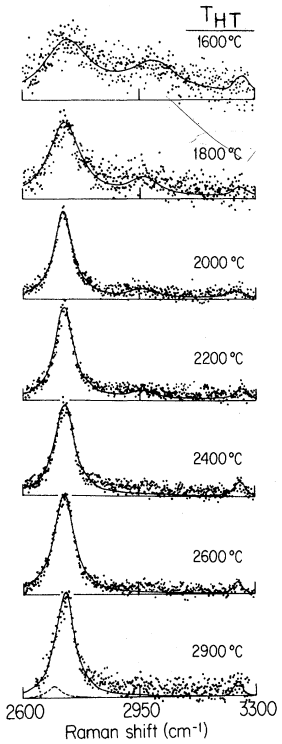

FIG. 6. Second-order Raman spectra for benzene-derived graphite fibers heat treated at various heat-treatment temperatures (T_{HT}). Increasing T_{HT} causes the dominant mode at ~ 2730 cm^{-1} to sharpen and causes an attenuation of the disorder-induced mode at ~ 2970 cm^{-1}. For $T_{HT}=2900$ °C, a shoulder near 2700 cm^{-1} in the 2730-cm^{-1} line (characteristic of highly ordered graphite) is barely visible.

2730-cm^{-1} mode above 2400 °C is not due to a broadening of the line but due to the appearance of an additional feature near 2700 cm^{-1} associated with the establishment of three-dimensional interplanar ordering. This additional feature causes the line shape of the 2730-cm^{-1} mode to become asymmetric, as shown in the trace at $T_{HT}=2900$ °C, the maximum T_{HT} value available in the present work. This doublet structure is partially resolved in HOPG and well resolved in single-crystal graphite,[10] and provides a sensitive probe for characterizing the onset of long-range three-dimensional ordering.[11,13,14]

In addition, another Raman band is observed between the two peaks at ~ 1360 and ~ 1580 cm^{-1} in the first-order spectra of the fibers. This additional structure is clearly seen in the samples heat treated at 1600 and 1800 °C (see Fig. 1), as an additional scattering intensity, beyond the superposition of Lorentzian fits to the two main first-order features.

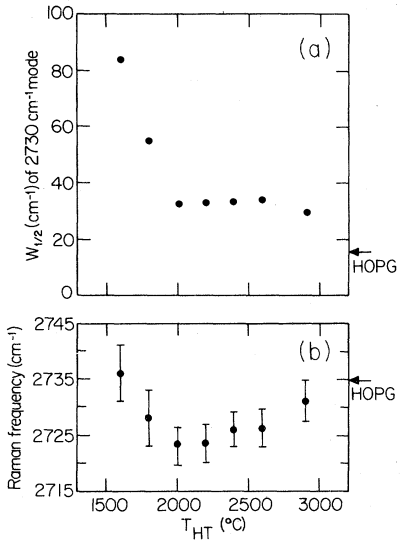

FIG. 7. (a) Halfwidth at half maximum (HWHM) linewidth and (b) peak mode frequency of the dominant line in the second-order Raman spectra at ~ 2730 cm^{-1} vs heat-treatment temperature (T_{HT}) for benzene-derived fibers. Corresponding linewidth and peak mode frequency for HOPG are also indicated.

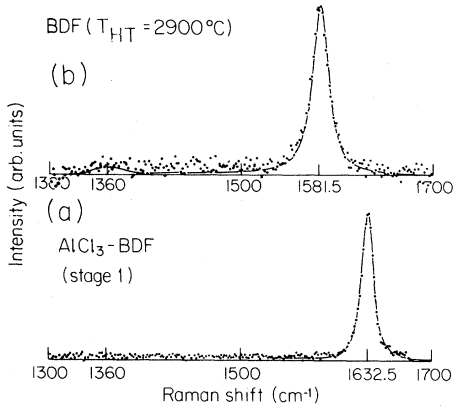

FIG. 8. (a) First-order Raman spectrum of a stage-1 $AlCl_3$-intercalated benzene-derived fiber in comparison to (b) that of the pristine fiber which was previously heat treated to 2900°C. This is the first reported observation of the Raman spectrum for a well-staged acceptor-intercalated graphite fiber.

This additional scattering band is observed to be dependent on T_{HT} and decreases rapidly as T_{HT} is increased up to 2000°C. Since the 1360- and 1620-cm^{-1} modes result from the small-crystallite-size effect and are associated with features in the density of vibrational states, it is possible that this extra scattering intensity is due to other features of the density of phonon states, as, for example, features between ~ 1360 and ~ 1580 cm^{-1} in the density of states.

To show that well-staged intercalated fibers can be prepared from the benzene-derived fibers, Raman spectra have been taken for donor and acceptor intercalated graphite fibers. The results in Fig. 8 for an $AlCl_3$-intercalated fiber, previously heat treated to 2900°C show clearly that a well-staged stage-1 acceptor compound can be prepared, based on the measured linewidth and mode frequency.[24] The peak frequency for stage-1 $AlCl_3$-intercalated graphite based on an HOPG host material is 1635 cm^{-1},[24] which is to be compared with 1632.5 cm^{-1} obtained for the benzene-derived fibers. The fiber was also characterized to be a well-staged first-stage compound using Debye-Scherrer x-ray measurements. The Raman linewidth (HWHM) for the stage-1 $AlCl_3$-intercalated fiber is 5.5 cm^{-1}, which is to be compared with a HWHM of 3 cm^{-1} for an HOPG-based sample. Although intercalation to stage 1 causes a dramatic increase in the fiber diameter, there is no evidence for intercalation-induced disorder, as indicated by the absence of structure at ~ 1360 cm^{-1} in the spectrum for the stage-1 $AlCl_3$-intercalated fiber (see Fig. 8). It is of interest to note that attempts to intercalate PAN GY70 and pitch UC4101B fibers with acceptor intercalants such as $AlCl_3$ and $FeCl_3$ did not yield staged compounds.[16]

The spectra in Fig. 9 taken for a Rb-intercalated fiber previously heat treated to 2900°C show two well-resolved lines associated with the graphite interior layers and the graphite bounding layers, with a HWHM of 6 and 7.5 cm^{-1} for the two lines, respectively, in comparison with 5.5 and 9.0 cm^{-1} for a Rb-intercalated HOPG sample.[25] The peak frequencies for the graphite interior-layer and bounding-layer modes are in good agreement with mode frequencies observed in Rb-intercalated HOPG samples, for a stage-5 or -6 compound, consistent with the mixed stage-5 and -6 pattern found from the (00l) lines on the Debye-Scherrer x-ray films. These Raman results obtained with intercalated fibers suggest that the benzene-derived fibers heat treated to high temperatures provide an excellent host material for intercalation studies. Further work is in progress on the Raman spectra for benzene-derived fibers intercalated with other donor and acceptor intercalants.

B. Resistivity measurements

Figure 10 shows the results of measurements of the room-temperature dc resistivity of single fibers

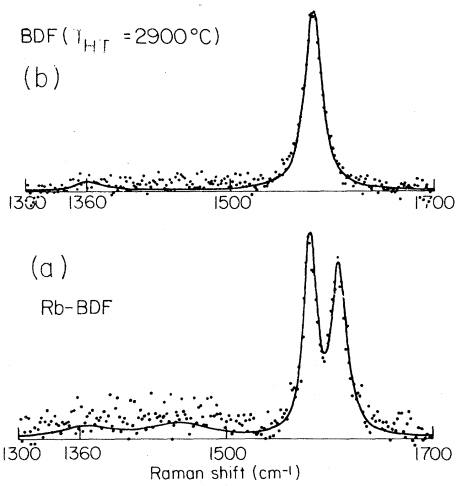

FIG. 9. (a) First-order Raman spectrum of a Rb-intercalated benzene-derived fiber in comparison to (b) that of the pristine fiber which was previously heat treated to 2900 °C. Trace for the intercalated fiber shows Raman lines for graphite interior and bounding layers (see text for a comparison of the linewidths for similar Raman spectra taken on HOPG-based intercalation compounds).

as a function of T_{HT}. As in the case of the Raman results, the curve in Fig. 10 exhibits three distinct regions of T_{HT} in the range $1200 < T_{HT} < 2900$ °C. The first nearly flat region for $1200 \leq T_{HT} \leq 2000$ °C, which is observed in most soft carbons, results from the compensation effect between crystalline growth and the decrease in carrier concentration.[26] The second region for $2000 < T_{HT} < 2600$ °C, characterized by a rapid decrease of the resistivity, corresponds to the establishment of long-range in-plane order, to a partial development of the three-dimensional graphite structure, and to an improvement in the preferred orientation of the crystallites. The third region ($2600 < T_{HT} < 2900$ °C) corresponds to the establishment of long-range three-dimensional ordering. The average resistivity at room temperature reaches ~ 70 $\mu\Omega$ cm for $T_{HT} \sim 2900$ °C. This value for the room-temperature resistivity is to be compared to ~ 40 $\mu\Omega$ cm for HOPG.[27] The lowest resistivity observed for any of the fibers heat treated to 2900 °C was 60 $\mu\Omega$ cm. The present resistivity results are qualitatively similar to results of previous resistivity studies on similarly prepared fibers.[6]

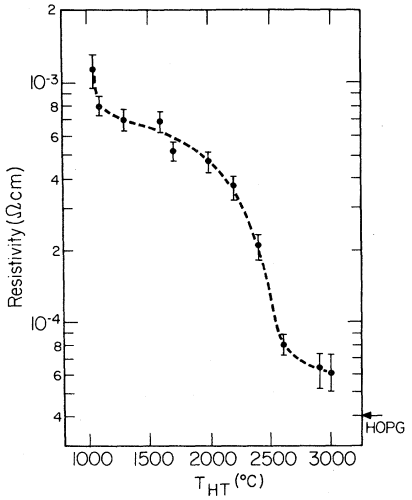

FIG. 10. Resistivity vs heat-treatment temperature (T_{HT}) of benzene-derived graphite fibers. Various features in the curve are identified with specific steps in the graphitization process (see text). For $T_{HT} = 2900$ °C, the resistivity is within 50% of that for HOPG.

The results of the resistivity measurements, which probe the bulk properties of the fibers, are consistent with the above Raman measurements, which probe mainly the near-surface regions of the fibers. Both results show approximately the same steps in the graphitization process and show that the present fibers exhibit a very high degree of graphitization. These resistivity results confirm that the benzene-derived fibers heat treated to 2900 °C and above have the highest crystallinity compared to any previously prepared fibrous carbon.

The high crystallinity of the benzene-derived fibers heat treated to 2900° C is also evidenced by the temperature dependence of the resistivity shown in Fig. 11. Generally, two types of temperature dependences are observed. Type I shows a monotonically slow increase of the resistivity with decreasing temperature from room temperature to liquid-helium temperature. Some samples heat treated to ~ 2900 °C exhibit type-I behavior which is characteristic of less-perfect fibers. The curve in Fig. 11 for the benzene-derived fiber labeled type II is representative of the second type, showing a shallow minimum in resistivity at ~ 220 K, a flat maximum at ~ 100 K, and a rapid falloff in the vicinity of liquid-helium temperature with a residual resistance ratio (RRR) $\rho_{300\,K}/\rho_{4.2\,K}$ of ~ 1.5. Most of the fibers heat treated to 2900 °C are of type II. The difference between these two types of fibers is attributed to differences in the degree of crystalline perfection of individual fibers. Also included in this figure is the temperature dependence of the resistivity of the pitch- and PAN-based fibers,[28] which do not show the metallic temperature dependence exhibited by the graphite whiskers[29] or single-

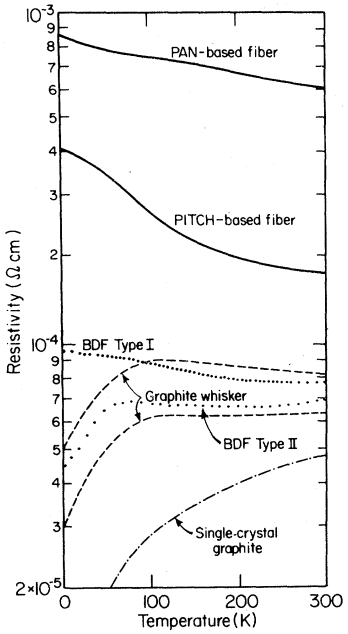

FIG. 11. Temperature dependence of the resistivity for type-I and -II benzene-derived graphite fibers heat treated to 2900 °C (see text) in comparison to the behavior of graphite whiskers, single-crystal graphite, and pitch- and PAN-based fibers. Decrease in resistivity below ~100 K indicates a high degree of ordering, insofar as the low-temperature resistivity is dominated by impurity and defect scattering, while at higher temperatures phonon scattering is dominant (see text).

crystal graphite.[30]

To determine the effect of intercalation on the transport properties of the benzene-derived fibers used for the Raman measurements, temperature-dependent resistivity measurements were carried out and the results are shown in Fig. 12, where the temperature dependence of $\log_{10}\rho$ is plotted for a dilute Rb-intercalated graphite compound and for a stage-1 $FeCl_3$-intercalated graphite compound. The figure shows that at room temperature intercalation with Rb and $FeCl_3$ results in a decrease in resistivity by factors of 9.3 and 10.1, respectively. The absolute values are comparable with values obtained with these intercalants on HOPG-based samples.[31] The resistivities achieved with these intercalants are within a factor of 4 that of copper at room temperature (1.8 $\mu\Omega$ cm), which was measured for reference with the same apparatus and measurement technique.

The results of Fig. 12 show a larger temperature dependence and a different functional form for the intercalated fibers than for the pristine fibers. However, the temperature dependence of the resistivity is roughly the same for the donor- and acceptor-intercalated fibers. $RRR = \rho_{300\,K}/\rho_{4.2\,K} = 5.7$ and 4.6 are found for the Rb- and $FeCl_3$-intercalated fibers, respectively. The RRR values measured here for acceptor-intercalated fibers are comparable to those found for acceptor-intercalated HOPG, but are more than an order of magnitude smaller than RRR values reported for stage-1 alkali-metal graphite intercalation compounds based on HOPG.[31]

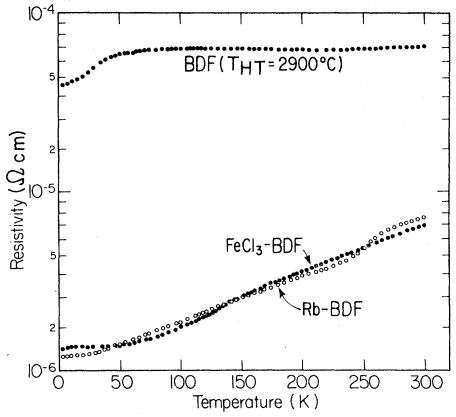

FIG. 12. Temperature dependence of the resistivity (plotted logarithmically) for benzene-derived graphite fibers (BDF), heat treated to 2900 °C, of a pristine fiber (top curve) and a Rb- and $FeCl_3$-intercalated fiber (curves labeled Rb-BDF and $FeCl_3$-BDF, respectively). These results represent the lowest resistivity values and the highest residual resistance ratios achieved to date in pristine and air-stable intercalated graphite fibers.

IV. DISCUSSION AND SUMMARY

Using both Raman scattering and resistivity measurements for the characterization of benzene-derived carbon fibers for crystalline order, it is concluded that both techniques can be used to provide complementary information on the various stages of graphitization of these fibers as the heat-treatment temperature is increased. These two techniques provide complementary information insofar as the Raman effect sensitively probes the optical skin depth (~600 Å), while resistivity measurements are sensitive to the bulk fiber. The results characteristically show the formation and growth of two-dimensional ordered regions, the onset of three-dimensional ordering, and finally the establishment of three-dimensional ordering. With regard to mode frequency and linewidth, the first-order Raman spectra for benzene-derived fibers heat treated

to 2900 °C are almost indistinguishable from that of HOPG. The second-order spectra do, however, show some differences, especially with regard to the linewidth of the 2730-cm^{-1} line and the shoulder on the low-frequency side of this line. The intensity ratio $R = I_{1360}/I_{1580}$ and the linewidth (HWHM) of the $\sim$1360-cm^{-1} line are especially sensitive to the nucleation of two-dimensionally ordered regions and their subsequent growth. The intensity ratio $R = I_{1360}/I_{1580}$ is also sensitive to the onset of three-dimensional ordering, as is the linewidth (HWHM) of the second-order line at 2730 cm^{-1}. The establishment of long-range three-dimensionally ordered regions is difficult to study by Raman spectroscopy since, for $T_{HT} \geq 2500$ °C, the first- and second-order Raman spectra rapidly approach those for HOPG or single-crystal graphite. The shoulder on the 2730-cm^{-1} second-order line is the most sensitive feature in the Raman spectra for the characterization of a very small amount of disorder.

The present results confirm that a highly graphitic and crystalline fiber can be prepared by heat treatment to 2900 °C. It is expected that further increases in crystalline order can be achieved by increasing the T_{HT} above 2900 °C, and such studies are now in progress. Heat treatments above 3000 °C are difficult because of sample vaporization and heat losses of the furnace, so that specially designed furnaces are needed.

Numerous uses of such highly crystalline fibers are expected both for practical applications and for carrying out new fundamental studies. The practical applications are likely to exploit the high tensile strength, high Young's modulus, and small diameters ($\sim$5000 Å) that can be achieved. Fundamental studies are also likely to exploit the availability of highly crystalline samples of very small diameter, greater than 1 cm in length and strong enough to be handled with tweezers. With these fibers it is also possible to prepare well-staged intercalation compounds. This is in fact the first report of a well-staged acceptor compound, prepared in a fiber host material. A larger temperature dependence with a different functional form is found for the intercalated fibers relative to that for the pristine fibers. It is of interest to note that resistivity values within a factor of 4 of copper are found for intercalated fibers at room temperature and residual resistance ratios of 5 are found upon cooling to 4.2 K. Since the benzene-derived fibers can be made with diameters down to 5000 Å, it is possible to carry out direct lattice-fringing studies of well-staged regions of an intercalation compound. Such lattice fringing of intercalated fibers is now under investigation.

ACKNOWLEDGMENTS

We wish to thank Dr. A. W. Moore of the Union Carbide Corporation for the HOPG and for assistance with the high-temperature anneals. We also thank Dr. G. Dresselhaus, Dr. R. L. Pober, and Dr. P. Kwizera for valuable discussions, and are grateful for NSF Grant No. DMR 78-24185 for support of the work done at MIT. One of the authors (M.E.) would like to express his thanks to Showa Denko Co., Ltd., for their encouragement of this work.

[1]T. Koyama, Carbon 10, 757 (1972).
[2]T. Koyama, M. Endo, and Y. Onuma, Jpn. J. Appl. Phys. 11, 445 (1972).
[3]M. Endo, T. Koyama, and Y. Hishiyama, Jpn. J. Appl. Phys. 15, 2073 (1976).
[4]M. Endo, A. Oberlin, and T. Koyama, Jpn. J. Appl. Phys. 16, 1519 (1977).
[5]T. Koyama, M. Endo, and Y. Hishiyama, Jpn. J. Appl. Phys. 13, 1933 (1974).
[6]T. Koyama and M. Endo, Jpn. J. Appl. Phys. 13, 1175 (1974).
[7]M. Endo, Y. Hishiyama, and T. Koyama, J. Phys. D 15, 353 (1982).
[8]F. Tuinstra and J. L. Koenig, J. Compos. Mater. 4, 492 (1970).
[9]P. Kwizera, A. Erbil, and M. S. Dresselhaus, Carbon 19, 144 (1981).
[10]R. J. Nemanich and S. A. Solin, Phys. Rev. B 20, 392 (1979).
[11]A. Marchand, P. Lespade, and M. Couzi, in *Extended Abstracts of the 15th Biennial Conference on Carbon, University of Pennsylvania, 1981,* edited by W. C. Forsman (University of Pennsylvania Press, University Park, Penn., 1981), p. 282.
[12]B. S. Elman, G. Dresselhaus, and M. Shayegan, in *Extended Abstracts of the 15th Biennial Conference on Carbon, University of Pennsylvania, 1981,* Ref. 11, p. 24.
[13]B. S. Elman, M. Shayegan, M. S. Dresselhaus, H. Mazurek, and G. Dresselhaus, Phys. Rev. B 25, 4142 (1982).
[14]B. S. Elman, M. S. Dresselhaus, G. Dresselhaus, E. W.

Maby, and H. Mazurek, Phys. Rev. B 24, 1027 (1981).
[15]P. Lespade, R. Al-Jishi, and M. S. Dresselhaus, Carbon (in press).
[16]P. Kwizera, M. S. Dresselhaus, and G. Dresselhaus, Carbon (in press); P. Kwizera, Ph.D. thesis, Massachusetts Institute of Technology, Cambridge, Massachusetts, 1981 (unpublished).
[17]L. B. Coleman, Rev. Sci. Instrum. 46, 1125 (1975).
[18]R. Al-Jishi, B. S. Elman, and G. Dresselhaus, in *Extended Abstracts of the 15th Biennial Conference on Carbon, University of Pennsylvania,* Ref. 11, p. 34.
[19]R. Al-Jishi and G. Dresselhaus, Phys. Rev. B 26, 4514 (1982).
[20]M. Maeda, Y. Kuramoto, and C. Horie, J. Phys. Soc. Jpn. 47, 337 (1979).
[21]P. C. Eklund, D. S. Smith, V. R. K. Murthy, and S. Y. Leung, Synth. Met. 2, 99 (1980).
[22]S. Y. Leung, G. Dresselhaus, and M. S. Dresselhaus, Phys. Rev. B 24, 6083 (1981).
[23]M. S. Dresselhaus and G. Dresselhaus, *Light-Scattering in Solids III,* Vol. 51 of *Topics in Applied Physics,* edited by M. Cardona and G. Güntherodt (Springer, Berlin, 1982), p. 3.
[24]G. M. Gualberto, C. Underhill, S. Y. Leung, and G. Dresselhaus, Phys. Rev. B 21, 862 (1980).
[25]S. A. Solin, Mater. Sci. Eng. 31, 153 (1977).
[26]S. Mrozowski, Phys. Rev. 85, 609 (1956).
[27]I. L. Spain, in *Chemistry and Physics of Carbon,* edited by P. L. Walker (Dekker, New York, 1973), Vol. 8, p. 1.
[28]P. Kwizera, M. S. Dresselhaus, and G. Dresselhaus, in *Extended Abstracts of the 15th Biennial Conference on Carbon, University of Pennsylvania, 1981,* Ref. 11, p. 100.
[29]R. Bacon, J. Appl. Phys. 31, 283 (1960).
[30]D. E. Soule, Phys. Rev. 112, 698 (1958).
[31]M. S. Dresselhaus and G. Dresselhaus, Adv. Phys. 30, 139 (1981).